The Astrophysical Journal, 667: L105–L108, 2007 September 20

MAGNETIC INTERACTION: AN ERUPTING FILAMENT AND A REMOTE CORONAL HOLE

Yunchun Jiang, Liheng Yang, Kejun Li, and Yuandeng Shen
National Astronomical Observatory/Yunnan Astronomical Observatory, Chinese Academy of Sciences, Kunming 650011, China; jyc@ynao.ac.cn
Received 2007 April 9; accepted 2007 July 27; published 2007 August 30

ABSTRACT

For the first time, we present a rare observation of direct magnetic interaction between an erupting filament and a coronal hole (CH). The small active region filament obliquely erupted toward the CH getting in the way, met and interacted with it, and then was deflected back. The erupting filament thus underwent a distinct to-and-fro motion in the visible disk, while the CH was clearly disturbed by the interaction. Brightenings in Hα and EUV and darkenings in He I 10830 Å appeared at the boundaries and in the interior of the CH. This eruption was closely associated with the initiation of a halo-type coronal mass ejection (CME). The direction of the CME, despite being greatly different from that of the initial filament eruption, was consistent with that of the reflected filament. Moreover, when the CME was seen in the limb, the filament was still in the process of the return journey in the visible disk. Therefore, it appears that the large-scale structure of the CME was bounced against and then reflected away from the CH along with the filament, and the eruptive filament represented only a very small part in the CME.

Subject headings: Sun: activity — Sun: coronal mass ejections (CMEs) — Sun: filaments — Sun: flares — Sun: magnetic fields — Sun: UV radiation

1. INTRODUCTION

The magnetic field plays a central role in defining the structure and dynamic in the solar corona. Different from numerous plasma magnetic loops that represent closed magnetic fields in active regions (ARs) and the quiet-Sun regions, coronal holes (CHs) are extended regions dominated by nearly unipolar magnetic fields that open into the heliosphere and generate high-speed solar wind streams (Zirker 1977). The CH boundaries thus form the separatrices between large-scale open and closed magnetic fields. CHs can be grouped into three broad categories: polar, nonpolar (isolated), and transient. They appear darker in X-ray and extreme ultraviolet (EUV) and brighter in the He I 10830 Å absorption line since they have densities and temperatures significantly lower than the typical background corona (Harvey 1996).

In the incessantly variable and magnetically dominant corona, it is possible that an erupting magnetic structure meets and interacts with other magnetic structures. Therefore, plasma and magnetic field interactions could take place over a wide range of scale and have been invoked to explain a broad form of solar activity. In particular, different kinds of magnetic interactions are considered to be involved in coronal mass ejections (CMEs), which represent the large-scale rearrangements of the coronal magnetic fields and are often associated with flares, filament eruptions, Moreton and EIT waves, and so on (Hudson & Cliver 2001). For instance, some observations have suggested that magnetic reconnection between open fields of CHs and adjacent closed fields along the CH boundaries can cause or facilitate some CMEs (Gonzalez et al. 1996; Lewis & Simnentt 2000); remote brightenings and dimmings in association with CMEs have been suggested as due to interaction of an erupting flux rope with overlying large-scale loops (Manoharan et al. 1996; Wang 2005; Jiang et al. 2006); and it is also found that a Moreton/EIT wave may interact with the ambient ARs or CHs and produces visible deflections as it propagates (Thompson et al. 1998, 1999; Veronig et al. 2006).

Observations of different types of magnetic interactions are therefore important in understanding the complex eruption process itself and the associated CME. It is not necessarily that a filament eruption should be radial. Thus, when a CH is in the way of the eruption, they will very likely meet and interact with each other. A rare event occurring on 2004 December 30 is just this case. Accompanied by a flare and a halo-type CME, a small AR filament obliquely erupted toward a CH and then directly ran up against it. As the first of a series, this Letter presents the first evidence for a new form of magnetic interaction occurring between the erupting filament and the CH.

2. OBSERVATIONS

The observations used in the present study include the following:

1. Full-disk Hα center and off-band (± 0.4 Å) images from the Air Force Improved Solar Observing Optical Network (ISOON; Neidig et al. 1998). The images have a cadence of 1 minute and a sampling of 1.1″ pixel^{-1}.
2. Full-disk He I 10830 Å intensity and velocity images from the Chromospheric Helium Imaging Photometer (CHIP; MacQueen et al. 1998) at the Mauna Loa Solar Observatory (MLSO). The CHIP data are acquired at seven filter positions covering the spectral region from 10826 to 10834 Å, which provides a measure of the line-of-sight velocity over the range of ± 100 km s^{-1} with an accuracy of approximately ± 5 km s^{-1} (Gilbert et al. 2001). The low corona white-light observations (1.08–2.85 solar radii) from the MLSO Mark IV (MK4) coronameter are also examined.
3. Full-disk EUV images with a pixel resolution of 2.6″, full-disk line-of-sight magnetograms with a pixel size of 2″ and a cadence of 96 minutes, and the C2 (C3) white-light coronagraph data that cover the range 2(4)–6(32) solar radii, from the Extreme Ultraviolet Telescope (EIT; Delaboudinière et al. 1995), the Michelson Doppler Imager (MDI; Scherrer et al. 1995), and the Large Angle and Spectrometric Coronagraph (LASCO; Brueckner et al. 1995) aboard the *Solar and Heliospheric Observatory* (*SOHO*), respectively. EIT 195 Å images were obtained continuously with a cadence of 12 minutes, while 171, 284, and 304 Å images were taken only once every 6 hr.

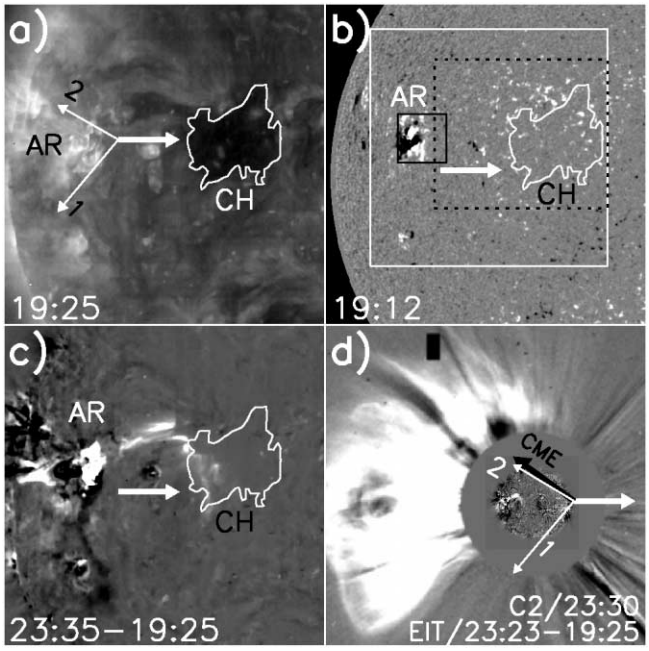

FIG. 1.—(*a*) EIT 195 Å direct image before the flare, (*b*) MDI magnetogram, (*c*) 195 Å difference image after the interaction, and (*d*) composite image of an inner EIT 195 Å with an outer LASCO C2 difference image. The CH boundaries determined from the 19:25 UT 195 Å image are superposed as white contours. The thick white (black) arrow indicates the initial eruption direction of the filament (the CME direction), and the thin white arrows indicate the ultimate directions of the two reflected filament legs. In (*b*), the white box indicates the FOV of Fig. 2*b*, and the black solid (dashed) box indicates the FOV of Fig. 2*a* (Fig. 3). The FOV is 1060″ × 1060″ for (*a*), (*b*), and (*c*).

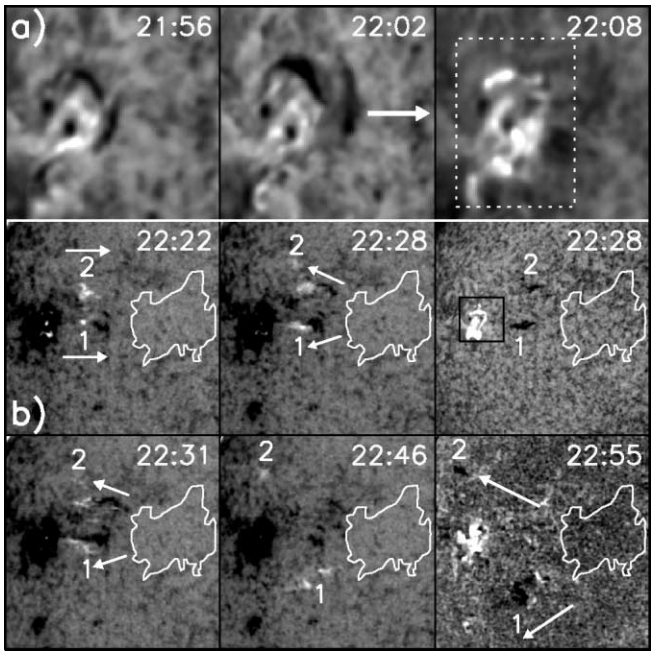

FIG. 2.—(*a*) ISOON Hα blue wing and (*b*) CHIP He I 10830 Å intensity images. In (*b*), Ha blue wing (*third panel*) and He I 10830 Å velocity (*last panel*) images are given. "1" and "2" mark the two legs of the erupting filament, and the arrows indicate their motion directions. The box in (*b*) indicates the FOV of (*a*), and the box in (*a*) indicates the area in which the Hα light curves are measured. The CH boundaries as in Fig. 1 are also plotted. The FOV of (*a*) is 160″ × 160″, and it is 780″ × 780″ for (*b*).

4. Full-disk soft X-ray (SXR) images with a resolution of 5″ pixel^{-1} from the Solar X-Ray Imager (SXI; Hill et al. 2005) aboard the *GOES-12* satellite. The SXI level-2 CH images created 4 times per day are examined.

3. RESULTS

The filament eruption occurred in AR 10715 and was followed by a flare of X-ray class M4.2 with start, peak, and end times around 22:02, 22:18, and 22:28 UT, respectively. A striking characteristic of the eruption is that the filament erupted toward the western direction, encountered an isolated CH standing in the way, and then was reflected back as two legs, "1" and "2" (see description below). The AR was centered at about N03°E48°, and the CH was to its due west, at about E13°N07° with longitudinal extension of about 18° from E24° to E06° and latitudinal width of roughly 13° from S01° to N12°, so the eastern CH boundary was 24° away from the AR. Figures 1*a* and 1*b* indicate that the CH was very close to the equator and predominantly had positive-polarity unipolar magnetic fields in the photosphere. After the eruption, the EIT 195 Å difference image in Figure 3*a* clearly shows that brightenings appeared at the boundaries and in the interior of the CH. A halo-type CME was observed to span the AR at about the flare time (see Fig. 1*d*). The MLSO MK4 movie shows that the CME front moved quite quickly through the low corona just above the east limb between 22:28 and 22:34 UT, and it was first seen in the field of view (FOV) of LASCO C2 at 22:30 UT. According to S. Yashiro's measurements, its center position angle (P.A.) was 54°. By applying second-order polynomial fitting, back extrapolation of the CME front from height-time (*H-T*) plots to the flare site yields an estimate of the onset time of the CME near 22:05 UT, which is very close to the start time of the *GOES* flare at 22:02 UT. Although the angle difference between the directions of the initial filament eruption and the CME determined by its center P.A. was about 144°, the ultimate direction of leg 2 was nearly along the CME direction, and the angular size subtended by the two reflected legs was approximately comparable with the angular extent of the brightest part of the CME. Such a temporal and spatial relationship indicates that the filament eruption and the flare were closely associated with the CME initiation.

The detailed eruption process of the filament is shown in Figure 2. Before the flare start, the small filament, located to the west of the AR, began to slowly rise at about 21:50. Then nearly at the same time as the flare start, it violently erupted toward the west direction (indicated by the white arrow in Fig. 2*a*). However, the filament did not immediately disappear but still ran a long distance after the flare end. This can be clearly discernible in Hα and He I 10830 Å images presented in Fig. 2*b* and broken down into the following consecutive stages. (1) From 22:22 to 22:28 UT, two finger-like branches, labeled "1" and "2," appeared between the AR and CH. They mainly showed blueshift signature and aimed at the CH. Thus, it seems that the erupting filament took the form of a rising Ω loop. The branches indicated its two legs when its top headed for the CH. Since the filament was close to the solar limb in the east hemisphere, taking the project effect into account, it appears that the filament did not erupt vertically but had an inclined path. Otherwise, the filament would leave the solar disk in the east direction. Similar inclined eruptions have also been shown by McAllister et al. (1996) and Jiang et al. (2007). (2) Next, the rising top approached and met with the CH boundaries. At 22:28 UT, when the flare ended, although the filament top was ambiguous in both Hα and He I images, which might be associated with ionizing and heating

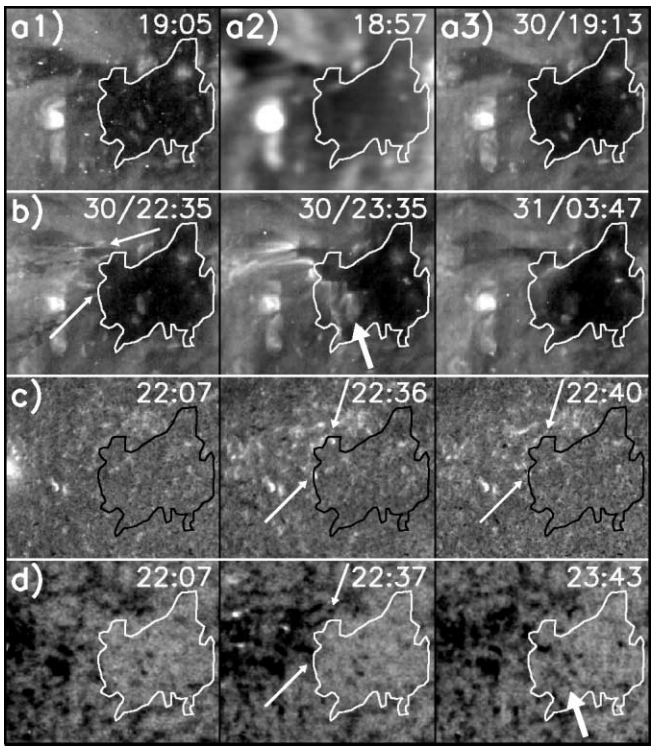

FIG. 3.—(*a*) EIT 284 Å (1), 195 Å (3), and SXI SXR (2) images showing the appearance of the CH before it met with the filament. Also shown are (*b*) EIT 195 Å, (*c*) ISOON Hα line center, and (*d*) CHIP He I 10830 Å intensity images. The thin arrows indicate the brightenings at the CH boundaries, and the thick arrows the brightenings in its interior. The CH boundaries as in Fig. 1 are also plotted. The FOV is 570″ × 490″.

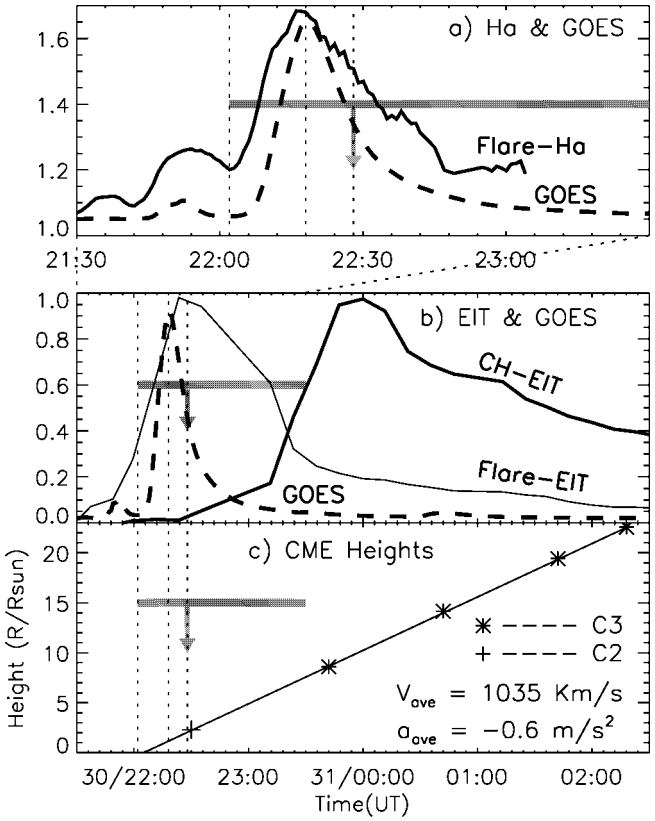

FIG. 4.—Time profiles of *GOES-12* 1–8 Å SXR (*dashed lines*), which are displayed in an arbitrary unit to fit in the panel. Also shown are the Hα center (*solid line in a*) and EIT 195 Å (*solid thin line in b*) flare light curves as a function of time in an area centered on the flare (indicated by the box in Fig. 2*a*) and 195 Å light curves in the CH area outlined by the contours in Figs. 1–3 (*solid thick line in b*). The value of 1.0 in Hα light curves indicates the mean Hα intensity outside the AR before the flare, and the 195 Å light curves are computed from the intensity integrated and normalized over these regions. (*c*) Heights of the CME front as the function of time and the back extrapolation by the use of second-order polynomial fitting. The arrows indicate the meeting time of the filament and the CH. The vertical bars indicate the start, peak, and end times of the flare, and the horizontal bars the duration of the to-and-fro motion of the filament in the visible disk.

of filament plasma, the two legs, especially leg 2, showed the earliest return signatures. Therefore, it appears that the meeting time was at this time, which was also confirmed by carefully examining the CHIP He I intensity movie. This gives an average projected speed of the filament rise of about 118 km s^{-1} between the flare start and the meeting. We see that the filament eruption was halted by the CH so could not pass through it. (3) The two legs then moved away from the CH, and eventually leg 1 (2) went beyond the east limb after about 23:30 (23:01) UT. Such returns were clearly visible in He I intensity and velocity images (see the 22:46 and 22:55 UT images in Fig. 2*b*) and not along the old trajectories. When the incoming legs were nearly parallel to the east-west direction, the outgoing legs had a large angular size, i.e., leg 1 (2) was along the northeast (southeast) direction (indicated by the white arrows). Moreover, the average return speed of leg 1 is estimated at about 143 km s^{-1}, which was slightly higher than the incoming speed. Therefore, it seems that the filament was snapped in two and reflected away from the CH after its top headed against the CH. These observations strongly suggest that interaction between the filament and CH indeed occurred. Owing to the obvious return signatures, we can pay attention to such interaction; otherwise, it will be difficult to directly relate the filament eruption to the remote CH.

Figure 3 shows the respondence of the CH to the interaction in 195 Å (Fig. 3*b*), Hα center (Fig. 3*c*), and He I 10830 Å intensity (Fig. 3*d*) images. Regarding 22:28 UT as the meeting time, the CH shows up as a dark region in EUV and SXR and as a bright region with similar shape in He I 10830 Å before the interaction. The changes of the CH due to the interaction were distinct. Weak brightenings (darkenings in He I 10830 Å) first appeared along the CH boundaries right-facing the incoming filament around 22:35 UT, which can be visible in all three wavelengths (indicated by the thin white arrows). Then the brightenings extended into the CH interior, reached their full extent about 1 hr after the meeting time (indicated by the thick white arrows), and slowly faded away in several hours. Note that such extension mainly occurred in the eastern part of the CH and was clearly discernible only in 195 Å and He I 10830 Å but not in Hα. The intrusion of the brightenings into the CH made its area shrink and its boundary be out of shape, possibly indicating that some changes and adjustments occurred in the open magnetic field of the CH. We believe that the brightenings represented another creditable manifestation of the interaction. In Figure 4, the light curves of EIT 195 Å intensities of the CH, and 195 Å and Hα intensities of the flare, are plotted and compared with *GOES* 1–8 Å SXR flux and the CME front *H-T* measurements; the average speed and acceleration of the CME front are also indicated. It is clear that the Hα and 195 Å flare light curves are approximately similar to the *GOES* SXR flux profile and the flare start time is consistent with the extrapolated CME onset time. The 195 Å intensities in the CH, however, show apparent increase only after the meeting time and reach maximum at about 23:48 UT, lagging the *GOES* flare maximum by about 90 minutes. It is noted that when the round trip of the erupting

filament did not end in the visible disk, the CME front already approached the outer edge of the C2 FOV.

4. CONCLUSIONS AND DISCUSSION

We present the observations of the direct interaction between the erupting filament and the CH. Two key factors make us believe that the interaction really occurred immediately after the filament collided with the CH. One is the return motion of the filament, definitely indicating that the filament was reflected away from the CH. The other is the chromospheric and coronal brightenings that appeared at the CH boundaries and then extended into its interior, obviously suggesting that the CH was disturbed by the hitting from the filament. Two magnetic systems were involved into such interaction: the magnetic fields of the filament and that of the CH. It is now well accepted that filament fields are usually dominated by the axis fields (Tandberg-Hanssen 1995), while CH fields are open into the heliosphere. Therefore, the inclined eruption indicated the filament fields had components normal to the CH fields. When the two magnetic systems collided with each other, the occurrence of interaction and reflections was an inevitable outcome, just like the case when a ball bumps against a wall and then springs back.

Our observations also revealed some important aspects of the filament eruption and its relationship with the CME. The filament eruption may be more complex than we imagined before. When the filament broke away from the magnetic restraint of the overlying corona arcade and from the magnetic tether of the barbs connecting it to the photosphere, sometimes it did not simply leave the Sun but was blocked by other magnetic features, the CH in this case, and so greatly altered its eruption direction. We would like to point out that such case was different from the "failing eruption" of a filament described by Ji et al. (2003) in which the overlying coronal field kept closing and the filament was still restrained below. On the other hand, when the CME was initiated by the filament eruption, its eruptive direction was greatly different from the initial direction of the filament eruption but consistent with that of the reflecting filament. Because the CME was first observed by the MK4 at 22:28 UT, when the filament was bounced against the CH, it is very likely that a significantly larger magnetic structure may be also bounced against the CH. Its upper portion was represented by the CME front, and its lower portion by the filament that broke but continued outward, ultimately in essentially the direction of the CME. Thus, the large-scale magnetic field restructuring associated with the CME may have a much larger spatial dimension than that of the erupting filament itself. In this case, we see that when the CME was in process, the erupting filament was still in the round trip with a long distance in the visible disk.

Our observations are very similar to the cases occurring between Moreton or EIT waves and CHs, which are reported by Thompson et al. (1998) and Veronig et al. (2006) and numerically studied by Wu et al. (2001). The waves can also stop at the CH boundaries, partially intrude into the CHs, and undergo strong reflection. The most significant difference is that the interaction studied here was due to the direct collision of the filament with the CH. We speculate that the brightenings in the CH interior may result from the filament material ramming into the CH, just like waves intruding into CHs during the wave/CH interactions. Because the filament was broken into two parts at its top, however, magnetic reconnection between the filament and the CH fields probably occurred, and the released energy may have flowed along the CH field line to produce the brightenings. If so, such reconnection at the CH boundaries, as found by some recent observations (Madjarska et al. 2004; Doyle et al. 2006), may be related with the slow solar wind (Wang 1998). To our knowledge, no theoretical study of these questions has been done. The detailed mechanism of the filament/CH interaction, which is still beyond the scope of our present observations, remains to be further understood.

The authors are grateful to an anonymous referee for many constructive suggestions and thoughtful comments, which improved the quality of this Letter. ISOON is operated by the Air Force Research Laboratory, Space Vehicles Directorate, at the National Solar Observatory, Sunspot, NM. He I 10830 Å data is provided by the High Altitude Observatory of the National Center for Atmospheric Research, which is sponsored by the National Science Foundation. We thank the SXI team and the *SOHO* MDI, EIT, and LASCO teams for data support. This work is supported by the Natural Science Foundation of China under grants 10573033 and 40636031 and by the 973 program (2006CB806303).

REFERENCES

Brueckner, G. E., et al. 1995, Sol. Phys., 162, 357
Delaboudinière, J.-P., et al. 1995, Sol. Phys., 162, 291
Doyle, J. G., Popescu, M. D., & Taroyan, Y. 2006, A&A, 446, 327
Gilbert, H. R., Holzer, T. E., Low, B. C., & Burkepile, J. T. 2001, ApJ, 549, 1221
Gonzalez, W. D., Tsurutani, B. T., McIntosh, P. S., & Clúa de Gonzalez, A. L. 1996, Geophys. Res. Lett., 23, 2577
Harvey, K. L. 1996, in AIP Conf. Ser. 382, Proc. Eighth International Solar Wind Conference, ed. D. Winterhalter et al. (New York: AIP), 9
Hill, S. M., et al. 2005, Sol. Phys., 226, 255
Hudson, H. S., & Cliver, E. W. 2001, J. Geophys. Res., 106, 25199
Ji, H., Wang, H., Schmahl, E. J., Moon, Y.-J., & Jiang, Y. 2003, ApJ, 595, L135
Jiang, Y. C., Li, L. P., Zhao, S. Q., Li, Q. Y., Chen, H. D., & Ma, S. L. 2006, NewA, 11, 612
Jiang, Y. C., Shen, Y. D., & Wang, J. X. 2007, Chinese J. Astron. Astophys., 7, 129
Lewis, D. J., & Simnentt, G. M. 2000, Sol. Phys., 191, 185
MacQueen, R. M., Blankner, J. G., Elmore, D. E., Lecinski, A. R., & White, O. R. 1998, Sol. Phys., 182, 97
Madjarska, M. S., Doyle, J. G., & van Driel-Gesztelyi, L. 2004, ApJ, 603, L57
Manoharan, P. K., van Driel-Gesztelyi, L., Pick, M., & Démoulin, P. 1996, ApJ, 468, L73
McAllister, A. H., Kurokawa, H., Shibata, K., & Nitta, N. 1996, Sol. Phys., 169, 123
Neidig, D., et al. 1998, in ASP Conf. Ser. 140, Synoptic Solar Physics, ed. K. S. Balasubramaniam, J. Harvey, & D. Rabin (San Francisco: ASP), 519
Scherrer, P. H., et al. 1995, Sol. Phys., 162, 129
Tandberg-Hanssen, E. 1995, The Nature of Solar Prominences (Dordrecht: Kluwer)
Thompson, B. J., Plunkett, S. P., Gurman, J. B., Newmark, J. S., St. Cyr, O. C., & Michels, D. J. 1998, Geophys. Res. Lett, 25, 2465
Thompson, B. J., et al. 1999, ApJ, 517, L151
Veronig, A. M., Temmer, M., Vršnak, B., & Thalmann, J. K. 2006, ApJ, 647, 1466
Wang, H. 2005, ApJ, 618, 1012
Wang, Y.-M. 1998, ApJ, 498, L165
Wu, S. T., Zheng, H., Wang, S., Thompson, B. J., Plunkett, S. P., Zhao, X. P., & Dryer, M. 2001, J. Geophys. Res., 106, 25089
Zirker, J. B. 1977, Coronal Holes and High Speed Wind Streams (Boulder: Colorado Associated Univ. Press)